Iranian Journal of Chemical Engineering

Journal Homepage: www.ijche.com

pISSN: 1735-5397
eISSN: 2008-2355

Regular Article

Assessing Nanostarch-Nanoclay Composite Films as Potentially Durable and Environmental-Friendly Packaging Materials

B. Momenpoor*[*], *F. Danafar, F. Bakhtiari, A. Namjoo

Department of Chemical Engineering, Faculty of Engineering, Shahid Bahonar University of Kerman, Kerman, Iran.

ARTICLE INFO

Article history:
Received: 2022-12-29
Accepted: 2023-11-12
Available online: 2023-11-12

Keywords:
Nanostarch,
Nanocomposite,
Corn starch,
Nanoclay,
Transparency

ABSTRACT

The properties of the Nanoclay-corn starch film were studied in the presence of Nanostarch. Nanostarch was synthesized through nanoprecipitation and characterized using the Particle Size Distribution Analysis, Field Emission Scanning Electron Microscopy (FESEM), X-ray diffraction Analysis (XRD), and Fourier Transform Infrared Analysis (FTIR). The XRD analysis of nanostarch particles revealed a distinctive V-type diffraction peak, with particle diameters ranging from 25 to 100 nm. The impact of introducing nanostarch into the starch-nanoclay film was investigated in terms of the thickness, transparency, morphology, wettability, and mechanical properties of the nanocomposite film. The results indicated that adding nanostarch particles improved the optical transparency of the film along with its hydrophobicity and flexibility. The film having a weight ratio of 0.769 (nanoclay to nanostarch) showed the maximum hydrophobicity (107.85°), and elongation at break (58.6%). This suggests that the appropriate incorporation of nanostarch can enhance the film's flexibility. The maximum tensile strength (5.88 MPa) was obtained for the film with a weight ratio of 1 (nanoclay to nanostarch).

DOI: 10.22034/ijche.2023.378569.1468 URL: https://www.ijche.com/article_182945.html

1. Introduction

Due to the huge demand for food and agricultural products, packaging technology has become much more important for these products. Fossil-fuel based polymers for packaging purposes have good mechanical

[*]Corresponding author: BehnazMomenpoor@gmail.com (B. Momenpoor)

properties to resist wear and tear but suffer from a long time to decompose. In this regard, improving the properties of the natural-based films for packaging has attracted research interests to reduce the environmental pollution caused by traditional synthetic polymer -based plastic food packaging [1].

Biopolymer based composites are favored in the packaging industry because of their biocompatibility, sustainability, and renewability as well as their low price. Starch is one of these biopolymers; which has poor resistance and mechanical properties compared to the synthetic polymer materials, thus limiting the use of starch-based composites[2]. One drawback to biocomposites is that their mechanical properties are sensitive to moisture. The absorbed moisture significantly reduces the mechanical properties of the composites. Further, the hydrophilicity of the film is important to retard the dehydration of the fresh wet products inside the package as well as to avoid moisture absorption by the dried product for keeping their crispness [3]. Nanostarch has attracted interest as a robust material for food packaging [4].

Researchers have shown that nanostructures like nanoclays [5,6], nanocellulose [7], nanostarch [8,9], and carbon nanotubes [10] significantly improve the mechanical properties of starch-based composites. The unique properties of nanostructures have revolutionized the composites science and engineering. Nanostructures usually by their large surface areas provide large interaction capacities, which make them capable of acting as important mechanical reinforcement loads [11]. Nanostructures because of their different morphologies, sizes and surface chemistiesy indicate different behaviors and thus affect the nanocomposite properties[12].

In particular, the reinforcing effect of nanostarch was evident from the tensile measurement of Kim et al [4], In most cases, the nanostarch causes an increase in both the tensile strength and elastic modulus of the composites but a decrease in elongation at the breakpoint. Li et al. studied the reinforcement of waxy maize starch nanocrystals in the pea starch-based film. They reported that increasing the content of starch nanocrystals (less than 5%) improved the measured values of tensile strength and elastic modulus in the nanocomposite [9].

In another study, the nanostarch was synthesized from mung bean through the same acid hydrolysis method which was also used for the preparation of starch-based films by the solution casting method. Different concentrations of nanostarch (0.5, 1, 2, 5 and 10%) were studied. The native starch film had the thickness of 0.040±0.010mm with the burst strength of 868.49±26.5 g. The rate of the water vapor transmission and water solubility were reported as 5.982×10^{-3} and 38.49±0.51% respectively Adding nanostarch at the concentration of 0.5 to 10.0% increased the film thickness from 0.043±0.006 to 0.063±0.006mm. Similarly, the burst strength of the film was enhanced from 943.56±18.1 to 1265±18.9g. Besides, the rate of the water vapour transmission and solubility decreased from $5.558 \times 10^{-3} \pm 0.25$ to $3.364 \times 10^{-3} \pm 0.35$g m^{-2} s^{-1} and 37.99±0.47 to 34.11±0.40% respectively [13].

Fazeli et al. synthesized nanostarch from corn starch through a precipitation method and employed the produced nanostarch for the fabrication of starch-based films. The results of this investigation indicated that adding starch nanoparticles led to improved mechanical properties and increased hydrophobicity[8].

Nanoclay is currently used as a major food packaging material available in market [14].

It significantly increases the resistance against water, improves mechanical properties and

decreases permeability of biopolymers [6]. The effects of nanoclays in human health are not well-known. There has been no conclusive evidence for negative effects of nanoclays on human health [5]. The current work focuses on embedding two types of nanostructures in starch to manipulate its mechanical properties and wettability. This research applies nanocomposites to hydrophobic films, which is relatively transparent and can bear large strains. To omit or minimize the amount of the nanoclay used as a filler, this study aims to develop a bio-based starch nanoparticles and prepare them as films on the packaging for food, medicine, cosmetics, etc.

The present work aims to evaluate the characteristic of a starch-nanocaly composite when nanostarch is added to it. The nanostarch used for the composite reinforcement was produced from corn starch using the simple and attractive method of nanoprecipitation. In this method, an aqueous suspension of a 2% (w/w) starch was added to a solvent system containing NaOH and urea. This mixture was agitated at a temperature of 35ºC for 60 mins and then added to ethanol for precipitation. The settled material was separated by centrifugation and washed with ethanol to remove any remaining solvents from the particles. The collected precipitate was finally air-dried under ambient conditions. The characteristics of the precipitate were investigated by SEM, FTIR, XRD and DLS methods. The produced nanostarch was used in the preparation of starch-based films containing different weight ratios of nanocaly to nanostarch. The transparency, wettability and mechanical properties of these films were studied using appropriate characterization techniques.

2. Materials and Methods

2.1. Materials

Native corn starch and nanoclay Cloisite (Na-Montmorillonite or Na–MMT, simply referred to as nanoclay in this paper) was used along with food grade glycerol as a plasticizer provided by Merck Company. Urea, sodium hydroxide and ethanol (96%) had reasonable purity and were used without further purification.

2.2. Preparation of Nanostarch

In the present work, nanostarch was produced from corn starch using the nanoprecipitation method described by Momenpoor et al [12]. In this method, an aqueous suspension containing 2%(w/w) starch was added to a solvent system in a 1:2 volumetric ratio. This mixture was then agitated at a temperature of 35ºC for 60 mins until it became a clear solution. The chosen solubilization temperature was intentionally lower than the gelatinization temperature of corn starch in water, which is typically between 62-72 ºC. The reason for using lower temperature is the solvent system included not only water but also NaOH and urea. The resulting solution was slowly added to ethanol at a ratio of 1/10 (by volume) under vigorous mechanical stirring. The mixture was then centrifuged at 5000 rpm for 30 mins. The liquid supernatant was separated, and the settled material was washed with 10 ml of ethanol to remove any remaining solvents from the particles. The collected precipitate was finally air-dried under ambient conditions.

2.3. Characterization of Starch and Nanostarch

2.3.1. Particle Size Distribution

The average size and size distribution of the nanostarch were considered by dynamic light scattering (DLS) instrument using a Malvern Zetasizer (Nano ZEN3600, Malvern Instruments Ltd., UK) equipped with a He-Ne laser (0.4 mW; 633 nm) and a temperature-controlled cell holder. The intensity of the

scattered light was detected at 90 ºC relative to the incident beam. The samples included a 0.1% wt/v nanostarch diluted in deionized water and analyzed at 25ºC [15].

2.3.2. Morphology Observation

The morphology of starch and nanostarch was investigated using a Field emission scanning electron microscope (TESCAN Model MIRA3). The nanostarch was mounted on circular aluminum stubs, then coated with gold, and the morphology was photographed at an accelerating voltage of 15 kVs.

2.3.3. Crystallinity

Starch is a biopolymer containing semi-crystalline granules with varying polymorphic types and degrees of crystallinity. The three-dimensional structural features of starch and nanostarch granules can be shown in X-ray diffraction patterns. (ASENWARE model AW-XDM300). XRD analysis was used to study the crystallinity change in nanostarch particles which may be produced during precipitation.

2.3.4. Structural Characteristics

Fourier transform infrared (FT-IR) (Brucker model TENSOR 27) spectroscopy was used for studying the structural characterization of starch and nanostarch. The samples were mixed with KBr to form a round disk suitable for FTIR measurements. The FTIR spectra were scanned over the wave number range of 4,000–400 cm^{-1}.

2.4. Starch Film Preparation

The determined amount of nanostarch according to Table 1 was added to deionized water (100ml) under intensive mixing for 10 min at 70°C. Then, the specific amount of nanoclay was added to the previous nanostarch suspension to obtain the desired percentages of nanostarch, nanoclay and mixed for 20 min. Corn starch and glycerol were separately mixed and then added to the suspension of starch/ clay nanoparticles

Table 1
Percentages of the materials in each film

Film number	Nanostarch	Nanoclay	Glycerol	Starch
1	1.8	1.8	25	71.4
2	2.3	1.8	25	70.9
3	2.8	1.8	25	70.4
4	3	0	25	72

The mixture was continuously stirred by a mechanical stirrer for 30 min at 70°C. The weight ratio of glycerol to corn starch was kept constant at 35% for all samples. The final solution was poured into polystyrene petri dishes and placed on a smooth surface in the laboratory to be dried under ambient condition (25 ± 2°C, 52 ± 3% RH). The advantages of adding nanostarch are when their amount is less than 5% [4].

All produced films were easy to handle and transparent. They were also easily removed from the surface of casting plates. All films based on visual observation, had smooth surfaces and showed good flexibility. The prepared films were characterized as described in the following sections.

2.5. Characterization of Starch Film

Formulations for four nanostarch dispersions were developed to produce films and show the

influence of the ratio of nanoparticles on the film characterization.

2.5.1. Thickness and Transparency

The thicknesses of the dried films were determined using an outside micrometer (0-25 µm) with an accuracy of ±0.01 mm. Ten thickness measurements were taken at different random locations of each film and the mean value of thickness for each film was reported in micron (µm). The mean thickness value of each film was used to calculate its tensile properties.

The starch film transparency was determined according to the method described by Ozdemir and Floros [16]. The films were cut into rectangular shapes (15 mm×50 mm) and optical transparency of films was derived by measuring light intensity using a spectrophotometer (LAMBDA25, Perkin Elmer, America). The specific wavelength of 560 nm used in the paper came from Heydari et al.[6]. Three replicates of each film were tested.

All tests were conducted at 23±2°C and 50±5% RH. The percentage of transparency was calculated using Equation 1.

$$TR\ (\%) = (I_r / I_0) \times 100 \quad (1)$$

where I_r is the light intensity with the specimen in the beam and I_0 is the reference light intensity.

2.5.2. Wettability and Morphology Observation

One droplet of deionized water was placed on the film surface to study the effects of nanoclay and nanostarch on the wettability. The close-view photos of both sides of water droplet were captured using an optical microscope. The initial contact angles in ten replications were measured using the ruler tool on the Adobe Photoshop CS5 (Adobe Systems, Inc., San Jose, CA) software.

Cross-section Micrographs of the films were obtained using a Field emission scanning electron microscope (TESCAN Model MIRA3), as outlined in section 2.3.2 in the context of nanostarch, it has been meticulously conducted.

2.5.3. Mechanical Properties

According to the standard ASTM method D 882-88, using a texture analyzer (TAPlus high-performance food texture analyzer, Lloyd Instruments) equipped with a 1 kN load cell, the mechanical properties of the films were analyzed by measuring the tensile strength and elongation at break. Tensile strength represents the maximal force per original cross-sectional area that the film can sustain before breaking, while elongation reflects the linear deformation of the material. Each sample was cut into rectangular strips (3 cm×8 cm). The machine was operated in the tensile mode with an initial grip separation of 40 mm and crosshead speed of 20 mm/min. Each sample was tested three times and the results were averaged. The E (%) was determined by dividing the extension at the rupture of the films by the initial length of the films (40 mm) multiplied by 100.

The TS was determined by dividing the maximum load (F) by the initial cross-sectional area (S) of the films (Eq. 2).

$$TS = F/S \quad (2)$$

where, TS: Tensile strength, (MPa), F: The maximum tensile force when the sample breaks, (N)

S: The initial cross-sectional area of specimen, m^2.

3. Results and Discussion

3.1. Characterization of Nanostarch

3.1.1. Particle Size Distribution of Nanostarch

The particle size and size distribution of nanostarch determined by DLS are presented in Fig. 1. The diameter of the nanostarch particles ranged from 25 to 100 nm. The curve has a single peak but indicates skewed toward the lower limit particle size distribution.

Compared to previous published literatures, the particle size and size distribution of nanostarch obtained in this study mostly (95%) lie between 25 and 58 nm. Qin et al. synthesized starch nanoparticles with 20–60 nm in size from corn starch with theprecipitation method [17].

The small-sized nanostarch has different physicochemical and mechanical properties compared to the large-sized nanostarch. Therefore, considering the high threshold of the particle size for small particles is important and necessary because it makes it possible to use them for the packaging in various pharmaceutical, cosmetic and food industries.

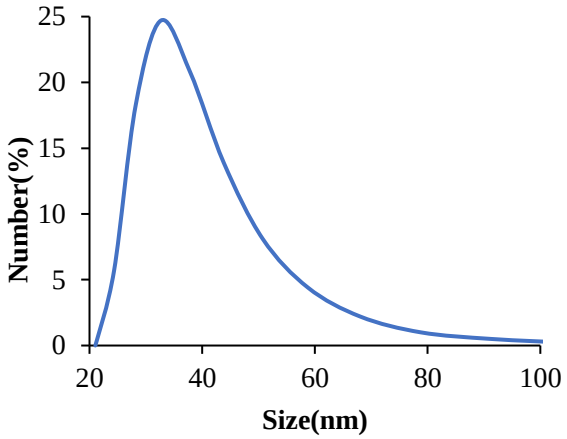

Figure 1. Particle size distribution of nanostarch produced by nanoprecipitation.

3.1.2. Morphology of Corn Starch Granules and Nanostarch

The morphology of corn starch, and nanostarch, prepared by precipitation, were scanned by SEM and FESEM respectively (Fig. 2). The corn starch (Fig. 2a) was observed to be mostly spherical or oval including some irregular granular shapes with a smooth surface and a range in diameter of about 2-30 µm when evaluated using SEM. According to Figure 1, cornstarch granules have different sizes and their average diameter is 15 µm. By dissolving the corn starch granules in an alkaline solution and then dropwise adding this dilute solution to a certain amount of ethanol, the nano-sized starch precipitated (Fig. 2b). As shown, most of nanostarch have an irregular morphology with aggregation.

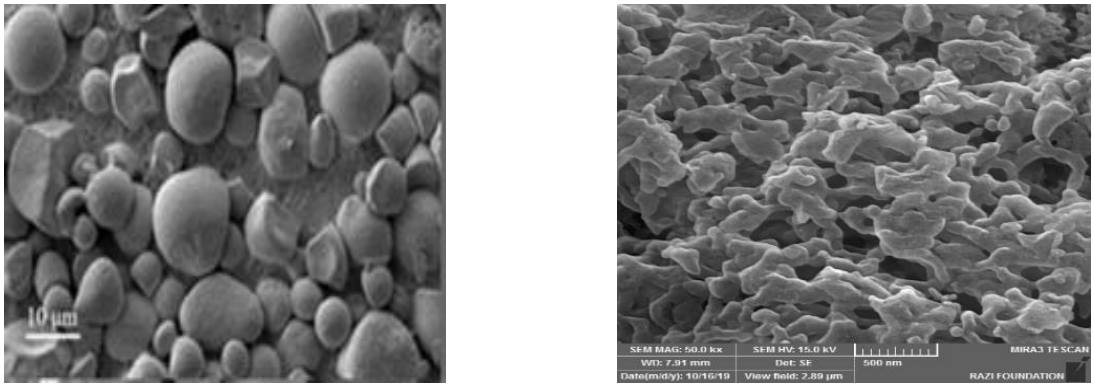

(a) (b)

Figure 2. Images of corn starch and nanostarch produced with nanoprecipitation, a) corn-starch, SEM; b) Nano-starch, FE-SEM.

3.1.3. X-ray of Corn Starch and Nanostarch

the crystallinity of starch is attributed to linear short chains presented in the amylopectin molecules and arrangement of these chains is reponsible for the three-dimensional crystalline structure; however, in starch films, the percentage of crystallinity depends on the amylose content of the starch [18]. During the film production process, first the starch is gelatinized and then retrogradation occurs, resulting in rearranged amylose molecules that lead to a more organized and crystallized structure of the amylose regions. With respect to the formation of the amorphous regions gathered through destroyed amylopectin regions, the amylose regions will be more sensitive to the effects of adding plasticizers. Hence, starch-based biodegradable films are transparent, odorless, tasteless and colorless.

The XRD diffraction patterns of the nanostarch sample compared to those of corn starch are shown in Fig. 3. The corn starch has the peaks of Bragg angles (2θ) at about 15 and 23°, and doublets at 17 and 18°, therefore it has the A-type diffraction pattern [19]. In the applications of starch nanoparticles, not only their sizes but also their crystalline structures are very important. For example, when used as fillers and reinforcements in nanocomposites, starch nanoparticles with higher crystallinity will improve the resistance and mechanical properties of the composites [20]. The XRD of nanostarch exhibits the V-type diffraction peak, which is observed at 17° while the diffraction peaks at 15, 18 and 23° completely vanish. As shown in Figure 3, as the particle size decreases, the diffraction peak becomes broader and the crystallite size becomes smaller. Also, the disappearance of the diffraction peak in the case of corn starch may be the consequence of the excessive decrease in the size of the crystallite due to the increase in the particle size.

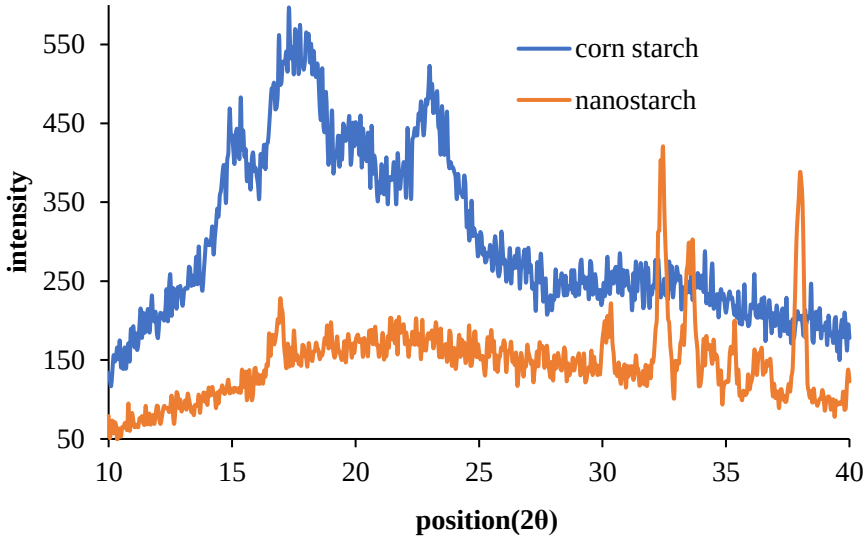

Figure 3. XRD analysis of corn starch and nanostarch produced by precipitation.

The gelatinized starch formed through dissolution of starch molecules in the alkaline solution destroyed the A-type crystallinity of corn starch, and the nanostarch precipitated in ethanol exhibited V-type crystallinity.

Therefore, in the nanostarch crystalline structure, the amylopectin cluster is destroyed and starch nanoparticles have more amorphous structures than starch. According to Ma et al., the V-type crystallinity has appeared in the plasticized corn starch [21].

3.1.4. FTIR Analysis of Nanostarch

The results of the FTIR spectrum are presented in Figure 4 to investigate the changes in the molecular structure of corn starch after the precipitation process. The FTIR spectrum for nanostarch reveals more peaks compared to the same for corn starch. The strong absorption band at 3485.42 cm^{-1} is related to the hydrogen bonded hydroxyl group stretching of starch.This wide band is limited to the complex vibrational stretching associated with the free inter and intra-molecular bound hydroxyl group and had strong absorption[22].

The O–H stretching vibration of starch and the N–H stretching vibration of urea are shown in the range of 3600 to 3100 cm^{-1} [23]. Hence, in nanostarch, O–H stretching vibrations might be overlapped with the N–H stretching vibration according to Figure 4 (that means some of the urea remains in the nanostarch). The C-H stretching correlated with the ring methane hydrogen atoms of corn starch and nanostarch is characterized by the band at 2917.94 cm^{-1}. The stretching and bending vibration of hydrogen bonding O–H groups of water is shown with the band of 1650.46 cm^{-1} [24]. To separate the OH bonds related to starch and water, the relevant peaks are assigned on Figure4.

Due to the strengthening of the C–OH bond, a strong absorption band at 1033.36 cm^{-1} is observed [25]. A strong O-H stretching band at 3485.42 cm^{-1} is observed in the corn starch, because of inter and intra-molecular bound hydroxyl groups. However, its intensity decreases in the spectra compared to that of nanostarch. Hebeish et al., also reported that the bands at 3435.7 cm^{-1} in the native corn starch decreased in intensity when compared to starch nanoparticles, due to inter and intra-molecular bound hydroxyl groups [22].

The band around 1644 cm^{-1} is related to the bending vibration of the water molecule, thus confirming the presence of water in the starch

[8]. However, its intensity decreases in the spectra compared to that of nanostarch. In general, when a water molecule is strongly interacting through hydrogen bonding, its bending vibration (H-O-H) requires a relatively higher energy to undergo vibrational excitation and vice-versa. As a result, the absorption wavenumber for the bending vibration of bound water in nanostarch is lower compared to the same vibration in starch molecules.

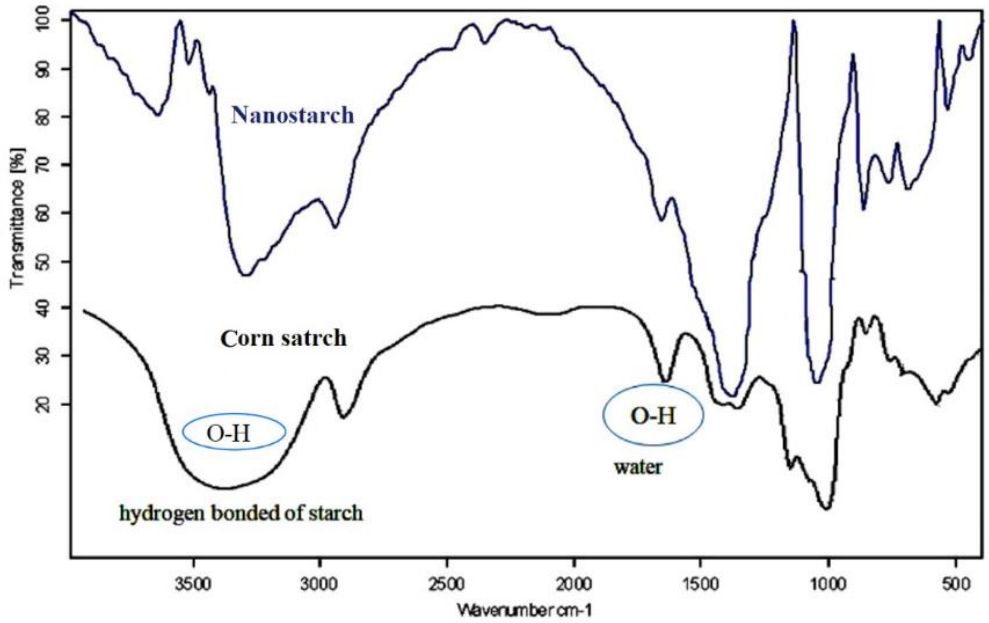

Figure 4. FTIR analysis of the corn starch and nanostarch produced by precipitation.

Therefore, according to the FTIR results, it can be said that starch with its both crystalline and amorphous regions interacts with the water in it. As a result, the extent of the hydrogen bonding interaction between the nanostarch and the bound water present in the system decreased. This is the reason for higher wave number shift of the –OH stretching vibration for nanostarch and lower wave number shift of the H-O-H bending vibration for bound water in starch nanocrystals.

3.2. Characterization of Starch Films

3.2.1. Thickness and Transparency

The thickness and transparency of the films are presented in Table 2. The film structure affects the thickness of the liquid film-forming dispersion which in turn influences the drying kinetics. Therefore, controlling the film structure is crucial for the physical and mechanical properties of the dried films.

The thickness of the films is directly proportional to the total mass of the material used. Consistent with Table 2, Li et al. reported that by increasing the nanostarch the film thickness increased [9]. To understand the reason for such observation, more study on the synergic effects of nanostructures and their interactions with the plasticizer and matrix is required.

Heydari et al. studied the effects of Na–MMT and glycerol on some functional properties of corn starch films [6]. The thickness of films with the same percent of materials, i.e., clay being 5% of the dry starch basis, plasticizer being 35% of the dry starch basis and the total amount of materials being 6.8 g, was obtained as 237.31 µm.

Table 2
Thickness and transparency of the films

Film number	Nanoclay/Nanostarch Ratio	Transparency (%)	Thickness (µm)
1	1	19.33	118.5
2	0.769	24.45	121
3	0.625	29.6	141
4	0	3.78	108.5

In this research, in addition to starch, glycerol and nanoclay, nanostarch was also used which increased the total mass. However, the thickness of all obtained films was smaller than that of films without nanostarch. In the production of nanostarch, the linear molecules of amylose, during the retrogradation process which occurs after gelatinization, changes and leads to a more organized and crystallized structure for amylose regions with respect to the amorphous formation gathered through destroyed amylopectin regions. Therefore, the rate of water absorbed decreases and the dehydration of the samples occurs in less time resulting in decreasing the thickness of the film with nanostarch.

The results indicated that the amount of nanostructure used is proportional to the film transparency. When the ratio of nanoclay/nanostarch decreased, the film transparency increases, however the film with no nanoclay had a minimum transparency. Nanostarch, which is a three-dimensional and crystalline nanostructure, has more effect on the film transparency. However, when there is no nanoclay, the film transparency significantly decreases.

The lowest transparency corresponds to the film 4, which does not have nanoclay. When there is no nanoclay in the film, the average percentage of nanoparticles decreases thereby decreasing the film transparency.

Hakke et al., studied the effects of the content of nanostarch on the properties of nanostarch/ polyurethane nanocomposites. Their results indicated that by increasing the concentration of nanostarch, the transparency of the films increased. These findings were in consistency with the results obtained from films 1, 2, and 3 in this study [26].

Maran et al. prepared tapioca starch-based edible films. Compared to this study, the transparency was lower [27]. Another observation, made from investigating the film thickness and transparency, was that there is no relationship between these two film characteristics. This implies that, although it is expected that a thicker film will show lower transparency, the transparency of the film with nanostructures does not depend on the film thickness.

As the particle size of a dispersion is reduced, Druffel et al. observed less light scatter [28]. The particle size must be limited to below 100nm to avoid excessive haze. Visible light is composed of wavelengths in the range of approximately 380–790 nanometers.

If nanoparticle with diameter of about one-tenth of the visible light wavelength is applied to the polymeric matrix, a transparent film with improved mechanical properties is produced. However, if nanoparticles were not well dispersed but agglomerated, they would become visible due to the increase in their size. The absorption properties and precise control of particle dimensions are the key parts of these systems. This requires the development of stable crystalline nanoparticle dispersions that do not agglomerate during the deposition and curing of the films. This will also further

stabilize the liquid formulations, resulting in improved shelf lives [28].

3.2.2. FTIR Analysis of Films

The covalent bonding of urea to starch was proven by FTIR spectrometry. Referring to Figure 5, for the case of using the two plasticizers (Urea and glycerol) the O–H stretching vibration of starch and glycerol and the N–H stretching vibration of urea are shown in the range of 3600 to 3100 cm^{-1} [23]. Hence, in film 4, the O–H stretching vibrations might be overlapped with the N–H stretching vibration (According to Figure 5).

Starch films plasticized only with glycerol, show the single peak centered at 3293 cm^{-1}, because of the stretching and bending vibrations of O–H groups [29]. Differently, three peaks around 3200, 3345, and 3452 cm^{-1} are observed for samples containing urea and glycerol, [29,30] because of the amide N–H symmetric and asymmetric stretching peaks of urea [29,31].

The band near 1637 cm^{-1} in starch has been attributed to the CH_2-bending absorption of starch overlapped by the absorption of moisture in the non-crystalline region [32]. This band becomes weaker as the crystallinity of the sample increases. The shift of this peak to a lower value (1616 cm^{-1}) indicates the N–H bending in the amide II region. More specifically the amide II band is derived mainly from the in-plane N–H bending and from the C–N stretching vibration [33].

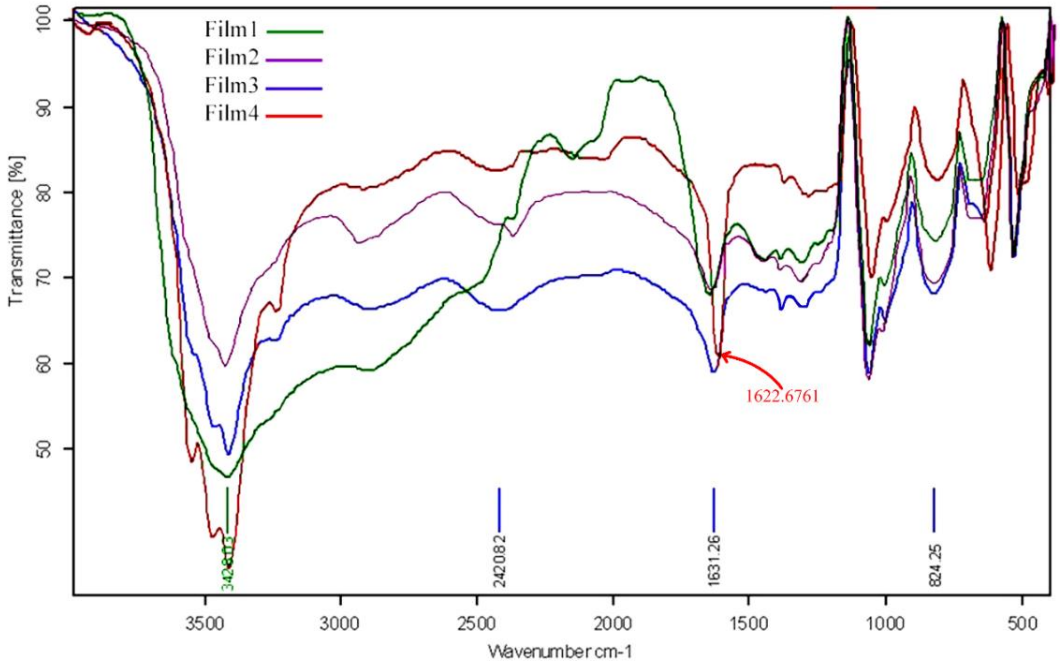

Figure 5. FTIR analysis of different films.

More especially the amide II band is resulted mainly from the C–N stretching vibration and in-plane N–H bending [34]. The bands at 1659 and 1626 cm^{-1} are attributed to the C=O stretching (amide I region) and N–H bending (amide II region) respectively [30]. In this study, urea was used for the synthesis of nanostarch, not as the plasticizer. Accordingly, the content of urea was low and the band at 1659 cm^{-1} did not appear. In the range of 1613-1688 cm^{-1}, the growing intensity of the peaks was observed due to the increase in the urea content. [22]. As shown in Figure 5, The

maximum intensity at 1688–1613 cm $^{-1}$ was for film 4, that has the maximum urea content. Menzel et al, studied the carbamation reaction between urea and starch. According to them, starch carbamates are produced above the melting point of urea (133 °C) through the decomposition of urea [34]. Their FTIR analysis confirmed the C=O stretching of the carbamate group (HNCOO) by the band at 1710 cm^{-1}. Here in, we did not notice this band in any of the spectra. Additionally, the findings in spectra suggest that there is no free urea in the samples, at least not in any significant amount. Zhou et al, have observed a peak at 1683 cm^{-1} due to the C=O vibration in the spectrum of the free urea[31].

3.2.3. Wettability and Morphology

A smaller contact angle between the film and water indicates a stronger attraction, leading to better adhesion between them.Conversely, a larger contact angle suggests a higher level of hydrophobicity in the biocomposite film [1].

The contact angle of each film is presented in table 3. By decreasing the nanoclay/nanostarch ratio, the contact angle increases from 84.8 to 107.85°. However, further decrease in the ratio causes a significant drop in the contact angle.

Table 3.
Water contact angel of different films

Film number	Contact angle (°)
1	84.82
2	107.85
3	66.75
4	43.5

Heydari et al., prepared films with starch, nanoclay and glycerol. The highest contact angle: 69.93 ° with 25% of glycerol and 5% of nanoclay [6].

Chen et al., prepared biocompisite films with corn nanostarch, glycerol and cellulose nanocrystal, and the most hydrophobic film had a contact angle of 58.5° [1]. Hybrid nanocomposite, with the suitable ratio of nanoparticles can have the highest hydrophobicity and thus better resistance property. The resistance to water vapor was improved, as indicated by the decreased angle when omitting the nanoclay. Furthermore, the role of nanoparticles on the hydrophobicity of the film is different. Nanoparticles increase the compactness of the films owing to their very small size.

Nanostarch can prevent the formation of inter-molecular hydrogen bonding amongst starch molecules which can reduce the water diffusion through the film [35].

Cross-sectional images of films 1 and 2, which have the highest hydrophobicity, are showed in Figure 6 with different resolutions. The films exhibited a homogenous phase, with large cohesiveness and minor porosity.

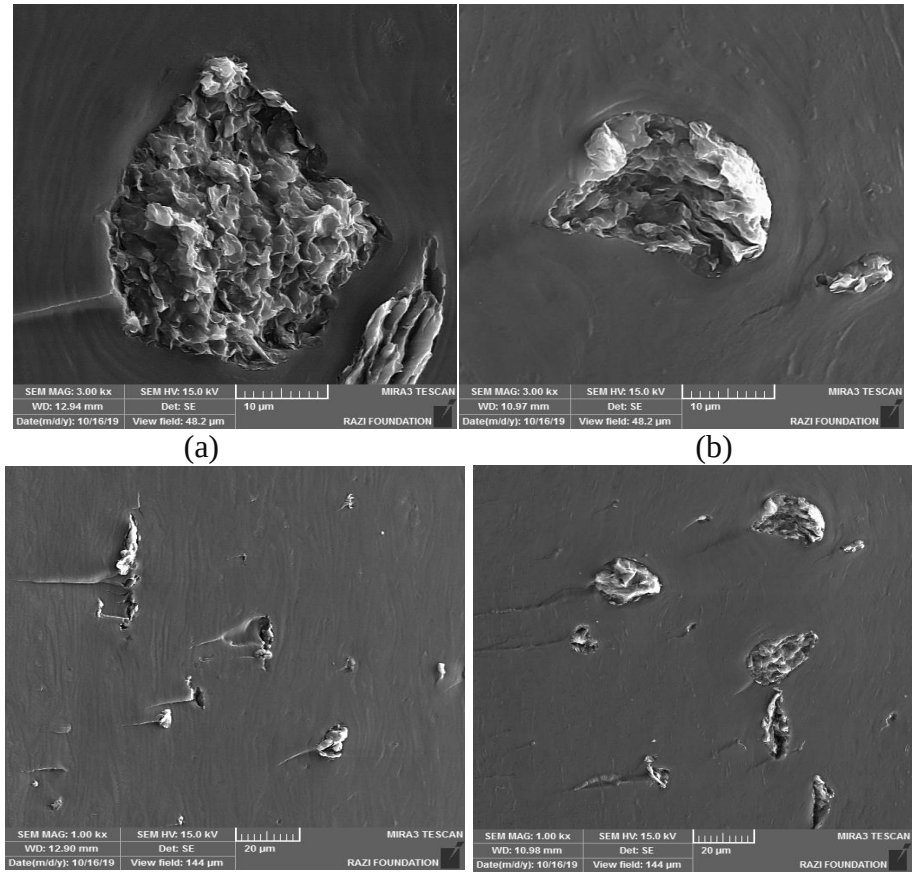

Figure 6. Cross-sectional field emission scanning electron microscopy (FESEM) images of the different films: a, c) film 1; b, d) film2.

As shown in figure 6, film-2 had more large sized pores than film-1, because of the aggregation of nanostarch arising from their inter-molecular interactions. While the film forming solution is dewatered to form films, owing to the driving force of water evaporation, numerous expanded starch granules and similar particles are randomly aggregated and compacted to form the films [11].

Similarly, Li et al, reported that there were obvious longitudinal ripples under the cross-section of the control films [9].These waves are transformed into transverse waves by the addition of nanostarch. This research team reported that when the amount of excess starch nanocrystals was 1%, the transverse fibrous structure of the composite layers was clearer at their cross-section, and as the starch nanocrystal content increased, more cracks appear.

In this study, the structure of the composite film's cross-section became more compact, maybe for the reason that the hydroxyl group on the nanostarch surface interacted with the hydroxyl group on the surface of corn starch. Similarly, when the hydroxyl group of the starch nanocrystals combined with that of pea starch through the hydrogen bonds the gel network structure formed [9]. The reason for the void forming may be that the nanoclay surface could not interact with the nanostarch and starch. The cross-sectional images of these samples captured by FESEM show a micro composite (phase separated composite), and the polymer chains have not penetrated the interlayer spacing of the nanoclay. These particles are aggregated.

3.2.4. Mechanical properties

Mechanical properties, including the tensile strength, percentage elongation, and Young's modulus, are crucial to packaging films . According to the conventional standards, the tensile strength of packaging films must be more than 3.5 MPa [36].

As shown in Table 4, all the obtained samples except the film without nanoclay have higher tensile strength. To study the effects of nanostach, the mechanical properties reported by Heydari et al have been added to Table 4. Similar to film-1, the glycerol was 35% and nanoclay was 2.5% of starch [6]. Comparing these two films, tensile strength increased by 80% and Young's modulus increased by more than 100%; whereas the elongation at break decreased by 60 %. Elongation at break indicates the flexibility of the film. Decreasing elongation at break will increase the film rigidity. As a typical reflection of ductility, the value of Young's modulus is higher when larger deformation occurs at an applied stress. Stiffness is how a component resists elastic deformation when a load is applied. Hardness is resistance to the localized surface deformation. The film deformation is related to the differences in stiffness between the matrix and the processing agents [11].

Nanostarch particles in an appropriate level can enhance the film flexibility. It plays a synergetic role in elongation at break due to its crystalline properties.

Film-2 had a maximum elongation at break while its Young's modulus and tensile strength were not the maximum. This is because when only nanostarch was used, the Young's modulus decreased significantly. In that case, the interface adhesion had not been enough to withstand the imposed high stretching forces, having resulted in diminished tensile strength. The highest amount of nanostarch induced an increase in both tensile strength and Young's modulus whereas the elongation at break decreased significantly. Nanoclays cause the stiffness to increase and nanostarch enhances elasticity. Nanostarch was not as influential as nanoclays in the strength of the composit. They displayed a lower tensile modulus but higher ultimate properties (strength and elongation at break). Therefore, depending on the application of the film, different ratios of nanostarch to nanoclay can be used.

Table 4
Results of tensile strength, elongation at break and Young's modulus.

Film number	Tensile strength (MPa)	Elongation at break (%)	Young's modulus (MPa)
1	5.88	33	305.17
2	4	58.6	106.62
3	5.68	13.03	352.66
4	1.134	23.46	13.68
Heydari et al. (2013)	3.29	83.78	57.26

The addition of plasticizers is basically required in order to obtain protein- and/or polysaccharides-based films. Plasticizers reduce cohesion within the film network by weakening the inter-molecular forces between adjacent polymer chains. In this way, plasticizers modify or improve the mechanical properties, increase the yield strength, hardness, density and viscosity, and increase the polymer chain flexibility as well as fracture strength. The use of natural plasticizers, like triglycerides from vegetable oils or fatty acid

esters, is increasing because they have low toxicity and low migration rates [3].

Due to a strong interaction between glycerol and starch, a hydrogen-bonding network is formed and a reinforced material is obtained. As the plasticizer content increases, the interactions between plasticizer and starch become stronger, resulting in swelling and a plasticization effect. At very high contents of plasticizer (above 50% w/w), starch becomes soft and behaves more like a gel or paste [37]. The addition of plasticizers, like glycerol, to edible films is required to overcome the film brittleness caused by extensive inter-molecular forces. Plasticizers also increase the mobility of polymer chains in addition to improving the flexibility and extensibility of the film. Here, glycerol as a plasticizer reduced the intra-molecular attraction between the starch chains by forming hydrogen bonds with starch molecules. The lesser the formation of hydrogen bonds between the starch chains, the greater the flexibility and subsequently the lower tensile strength [6]. It is important to recall that the proportional amount of starch to plasticizer (glycerol) was fixed in this study.

Nanostarch has a highly reactive surface with plenty of hydroxyl groups. Glycerol in combination with nanostarch can impart a high degree of binding between the nanoparticles and starch molecules to improve the nanoparticle-starch interface and promote individualization.

4. Conclusion

Starch and clay nanostructures were used to improve the mechanical properties of starch-based films. A unique combination of two nanomaterials was highly effective in overcoming certain limitations of nanocomposites, which uses only one type of nanomaterials. This type of hybrid nanocomposites is expected to be useful in developing eco-friendly polymer nanocomposites with superior properties. It was shown that different ratios of nanoclay/ nanostarch can be used to improve the transparency of the films with the thicknesses values up to several microns, while simultaneously increase its mechanical characteristics. The transparency of the films improves by decreasing the nanoclay to nanostarch ratio. The addition of these nanomaterials also enhances the film hydrophobicity considerably.

The film with the nanoclay/nanostarch ratio of 0.769 showed maximum hydrophobicity and elongation at break, as well as maximum flexibility. Whereas, film-1 had the maximum tensile strength, and the contact angle was 84.82°. The advantage of using nanostarch in the films to increase hydrophobicity, tensile strength and Young's modulus. Accordingly, these films can play important roles in applications requiring high wettability and mechanical flexibility. However, more research is required to understand the complex plasticizer/matrix/nanofiller interactions and their influence on the resulting mechanical properties of the composite.

References

[1] Chen Q, Zhou L, Zou J, Wang J. “Response Surface Optimization of Process Conditions and Characteristics of Nanostarch-based Biocomposite Film Reinforced by Cellulose Nanocrystals”. BioResources.;14(2),4344, (2019).

[2] Adeyeye, S.A.O., Babu, A.S., Guruprasath, N. and Ganesh, P.S. “Starch Nanocrystal and its Food Packaging Applications”. *Current Research in Nutrition and Food Science Journal*, *11*(1), pp.01-21,(2023).

[3] Cazón P, Velazquez G, Ramírez JA, Vázquez M. “Polysaccharide-based films and coatings for food packaging: A

review". Food Hydrocolloids. 68,136-48, (2017).

[4] Kim, H. Y., Park, S. S., & Lim, S. T. "Preparation, characterization and utilization of starch nanoparticles. *Colloids and Surfaces B" Biointerfaces*, *126*, 607-620, (2015).

[5] Barzegar, H., Azizi, M. H., Barzegar, M., & Hamidi-Esfahani, Z. "Effect of potassium sorbate on antimicrobial and physical properties of starch–clay nanocomposite films". *Carbohydrate polymers*, *110*, 26-31, (2014).

[6] Heydari, A., Alemzadeh, I., & Vossoughi, M. "Functional properties of biodegradable corn starch nanocomposites for food packaging applications". *Materials & Design*, *50*, 954-961, (2013).

[7] Pelissari, F. M., Andrade-Mahecha, M. M., do Amaral Sobral, P. J., & Menegalli, F. C." Nanocomposites based on banana starch reinforced with cellulose nanofibers isolated from banana peels". *Journal of colloid and interface science*, *505*, 154-167, (2017).

[8] Fazeli, M. and Lipponen, J., 2022. "Developing Self-Assembled Starch Nanoparticles in Starch Nanocomposite Films". *ACS omega*, *7*(49), pp.44962-44971,(2022).

[9] Li, X., Qiu, C., Ji, N., Sun, C., Xiong, L., & Sun, Q. "Mechanical, barrier and morphological properties of starch nanocrystals-reinforced pea starch films". *Carbohydrate polymers*, *121*, 155-162, (2015).

[10] Cheng, J., Zheng, P., Zhao, F., & Ma, X. "The composites based on plasticized starch and carbon nanotubes". *International Journal of Biological Macromolecules*, *59*, 13-19, (2013).

[11] Santana, J. S., de Carvalho Costa, É. K., Rodrigues, P. R., Correia, P. R. C., Cruz, R. S., & Druzian, J. I. "Morphological, barrier, and mechanical properties of cassava starch films reinforced with cellulose and starch nanoparticles". *Journal of Applied Polymer Science*, *136*(4), 47001, (2019).

[12] Sharifzadeh, E., Tohfegar, E. and Safajou Jahankhanemlou, M."The influences of the nanoparticles related parameters on the tensile strength of polymer nanocomposites". *Iranian Journal of Chemical Engineering (IJChE)*, *17*(1), pp.65-78,(2020).

[13] Roy, K., Thory, R., Sinhmar, A., Pathera, A.K. and Nain, V. "Development and characterization of nano starch-based composite films from mung bean (Vigna radiata)". *International journal of biological macromolecules*, *144*, pp.242-251,(2020).

[14] Adeyeye, S. A. O., & Ashaolu, T. J. "Applications of nano- materials in food packaging: A review". *Journal of Food Process Engineering*, *44*(7), e13708, (2021).

[15] Momenpoor, B., Danafar, F., & Bakhtiari, F,"Size Controlled Preparation of Starch Nanoparticles from Wheat Through Precipitation at Low Temperature". In *Journal of Nano Research* , 56, pp. 131-141, (2019).

[16] Ozdemir, M., & Floros, J. D. "Optimization of edible whey protein films containing preservatives for mechanical and optical properties". *Journal of Food Engineering*, *84*(1), 116-123, (2008).

[17] Qin, Y., Liu, C., Jiang, S., Xiong, L., & Sun, Q. "Characterization of starch nanoparticles prepared by nanoprecipitation: Influence of amylose content and starch type". *Industrial Crops and Products*, *87*, 182-190, (2016).

[18] García, M. A., Martino, M. N., & Zaritzky, N. E. "Microstructural characterization of plasticized starch-based films". *Starch- Stärke*, *52*(4), 118-124, (2000).

[19] Sun, Q., Gong, M., Li, Y., & Xiong, L. "Effect of dry heat treatment on the physicochemical properties and structure of proso millet flour and starch". *Carbohydrate polymers*, *110*, 128-134, (2014).

[20] Yan, X., Chang, Y., Wang, Q., Fu, Y., Ren, L., & Zhou, J. "Influence of precipitation conditions on crystallinity of amylose nanoparticles". *Starch-Stärke*, *70*(7-8), 1700213, (2018).

[21] Ma, X., Jian, R., Chang, P. R., & Yu, J. "Fabrication and characterization of citric acid-modified starch nanoparticles/plasticized-starch composites". *Biomacromolecules*, *9*(11), 3314-3320, (2008).

[22] Hebeish, A., El-Rafie, M. H., El-Sheikh, M. A., & El-Naggar, M. E. "Ultra-fine characteristics of starch nanoparticles prepared using native starch with and without surfactant". *Journal of Inorganic and Organometallic Polymers and Materials*, *24*(3), 515-524, (2014).

[23] Rychter, P., Kot, M., Bajer, K., Rogacz, D., Šišková, A., & Kapuśniak, J. "Utilization of starch films plasticized with urea as fertilizer for improvement of plant growth". *Carbohydrate polymers*, *137*, 127-138, (2016).

[24] Lammers, K., Arbuckle-Keil, G. and Dighton, J."FT-IR study of the changes in carbohydrate chemistry of three New Jersey pine barrens leaf litters during simulated control burning". *Soil Biology and Biochemistry*, *41*(2), pp.340-347,(2009).

[25] Černá, M., Barros, A. S., Nunes, A., Rocha, S. M., Delgadillo, I., Čopíková, J., & Coimbra, M. A. "Use of FT-IR spectroscopy as a tool for the analysis of polysaccharide food additives". *Carbohydrate Polymers*, *51*(4), 383-389, (2003).

[26] Hakke, V.S., Landge, V.K., Sonawane, S.H., Babu, G.U.B., Ashokkumar, M. and Flores, E.M., "The physical, mechanical, thermal and barrier properties of starch nanoparticle (SNP)/polyurethane (PU) nanocomposite films synthesised by an ultrasound-assisted process". *Ultrasonics Sonochemistry*, *88*, p.106069,(2022).

[27] Maran, J. P., Sivakumar, V., Sridhar, R., & Thirugnanasambandham, K. "Development of model for barrier and optical properties of tapioca starch based edible films". *Carbohydrate polymers*, *92*(2), 1335-1347, (2013).

[28] Druffel, T., Buazza, O., Lattis, M., Farmer, S., Spencer, M., Mandzy, N., & Grulke, E. A. "The role of nanoparticles in visible transparent nanocomposites". In *Nanophotonic Materials V* 7030, pp. 66-74, (2008).

[29] Versino, F., Urriza, M., & García, M. A. "Eco-compatible cassava starch films for fertilizer controlled-release". *International journal of biological macromolecules*, *134*, 302-307, (2019).

[30] Wang, J. L., Cheng, F., & Zhu, P. X. "Structure and properties of urea-plasticized starch films with different urea contents". *Carbohydrate polymers*, *101*, 1109-1115, (2014).

[31] Zhou, T., Wang, Y., Huang, S., & Zhao, Y. "Synthesis composite hydrogels from inorganic-organic hybrids based on leftover rice for environment-friendly controlled-release urea fertilizers". *Science of the Total Environment*, *615*, 422-430, (2018).

[32] Santha, N., Sudha, K. G., Vijayakumari, K. P., Nayar, V. U., & Moorthy, A. S. "Raman and infrared spectra of starch samples of sweet potato and cassava". *Journal of Chemical Sciences*, *102*(5), 705-712, (1990).

[33] Kong, J., & Yu, S. "Fourier transform infrared spectroscopic analysis of protein secondary structures". *Acta biochimica et biophysica Sinica*, *39*(8), 549-559, (2007).

[34] Menzel, C., Seisenbaeva, G., Agback, P., Gällstedt, M., Boldizar, A., & Koch, K. "Wheat starch carbamate: Production, molecular characterization, and film forming properties". *Carbohydrate Polymers*, *172*, 365-373, (2017).

[35] Shi, A. M., Wang, L. J., Li, D., & Adhikari, B. "Characterization of starch films containing starch nanoparticles: Part 1: Physical and mechanical properties". *Carbohydrate Polymers*, *96*(2), 593-601, (2013).

[36] Kim, Y. J., Lee, H. M., & Park, O. O. "Processabilities and mechanical properties of surlyn- treated starch/LDPE blends". *Polymer Engineering & Science*, *35*(20), 1652-1657, (1995).

Bertolini, A. (Ed.). "*Starches: characterization, properties, and applications"*. CRC Press, (2009).